

# Influence of Initial Bubble Size on the Dynamic Behavior of Fluid in a DAF Tank

Jingming Li<sup>1,\*</sup>, Jiahui Xu<sup>2</sup>, Zhaodong Huang<sup>3</sup>, Yadi Wang<sup>4</sup>

<sup>1</sup>College of New Energy, Xi'an Shiyu University, Xi'an 710043, China

<sup>2</sup>College of Mechanical Engineering, Xi'an Shiyu University, Xi'an 710043, China

<sup>3</sup>College of Mechanical Engineering, Xi'an Shiyu University, Xi'an 710043, China

<sup>4</sup>College of Mechanical Engineering, Xi'an Shiyu University, Xi'an 710043, China

\* Corresponding author

**Abstract:** To explore the impact of non-uniform initial bubble sizes on the hydrodynamics behavior of the separation zone in a dissolved air flotation (DAF) tank, a three-dimensional (3D) model of the DAF tank was established. Subsequently, computational fluid dynamics (CFD) simulations of the corresponding DAF tank were conducted based on the realizable  $k-\epsilon$  turbulence model, the Eulerian-Eulerian multiphase flow model, and the population balance model (PBM). The reliability of the prediction results of the 3D model was evaluated by comparing the gas holdup and velocity vector data obtained from experimental results. Moreover, considering the coalescence and breakage of bubbles, the influence of different initial bubble sizes on the variation trend of the gas holdup with height in the separation zone of the DAF tank was analyzed when different flotation media, namely air, carbon dioxide, were adopted. The study reveals that as the density of the flotation medium increases, the optimal size range of the initial bubbles also gradually expands. Specifically, when air and carbon dioxide are used as the flotation media, the optimal ranges of the initial bubble sizes are 25-50  $\mu\text{m}$  and 25-75  $\mu\text{m}$ , respectively.

**Keywords:** Initial bubble size, dissolved air flotation, population balance model, simulation.

## 1. Introduction

With the continuous growth of the global population and the advancement of urbanization, the contradiction between increasing urban water demand and limited water resources has become increasingly prominent. Concurrently, the discharge of industrial wastewater and domestic sewage has led to deteriorating water quality, posing significant challenges to urban water supply security. To address these challenges, effective treatment of wastewater for reuse has emerged as a critical approach to ensuring urban water supply safety and maintaining environmental health. However, conventional water treatment methods exhibit certain limitations in removing contaminants such as ions, colloids, emulsified oils, and ultrafine particles, necessitating more efficient solutions<sup>[1]</sup>. As an emerging water treatment technology, dissolved air flotation (DAF) has gained widespread application<sup>[2]</sup>.

Dissolved air flotation (DAF) removes contaminant particles from water by utilizing microbubbles as a separation medium. The process involves dissolving gas into water under high pressure to form a saturated solution, which is then introduced into the flotation tank for pressure release. Upon sudden depressurization, the dissolved gas precipitates as fine bubbles that attach to suspended flocs, forming bubble-floc aggregates. Due to density differences, these aggregates rise to the surface, accumulate as a foam layer, and are subsequently removed by a skimming device<sup>[4-5]</sup>.

The flotation tank is typically divided into two functional zones: the contact zone and the separation zone. The tank's structural design is a critical factor influencing hydrodynamic behavior and, consequently, separation efficiency. Extensive research has been conducted in this field. Kwon et al.<sup>[6]</sup> developed a flotation tank model and demonstrated through simulations that the aspect ratio significantly affects the

working zone and microbubble size distribution—a finding later validated by ADV measurements. Tang et al.<sup>[7]</sup> employed numerical simulations to investigate the impact of separation zone length and tank height on flotation efficiency, revealing that efficiency increases with separation zone length but decreases with the height difference between the tank and baffle, consistent with theoretical predictions. Berrio et al.<sup>[8]</sup> designed a novel flotation tank structure that outperforms conventional designs in efficiency while reducing energy and resource consumption. Wang et al.<sup>[9]</sup> developed a countercurrent-concurrent dissolved air flotation (CCDAF) process; simulations indicated that, compared to conventional co-current and countercurrent DAF systems, the CCDAF process reduces effluent turbidity by 5.0% and 8.8% under single-phase, gas-liquid two-phase, and varying gas holdup conditions, demonstrating superior flow field characteristics and enhanced contaminant removal.

Initial bubble size plays a crucial role in flotation efficiency. Studies suggest optimal performance when the average bubble diameter is around 40  $\mu\text{m}$ <sup>[10]</sup>. Deng et al.<sup>[11]</sup> simulated gas-phase distribution characteristics for bubble diameters of 40  $\mu\text{m}$ , 80  $\mu\text{m}$ , and 120  $\mu\text{m}$  (neglecting coalescence and breakup effects) and found that larger bubbles tend to escape from the top of the separation zone more readily, whereas smaller bubbles exhibit stronger adhesion to flocs. Chen et al.<sup>[12]</sup> employed an Euler-Euler model to analyze the behavior of 30–70  $\mu\text{m}$  bubbles, revealing that larger bubbles promote stratified flow. The stratification effect becomes more pronounced as bubble diameter increases from 30  $\mu\text{m}$  to 50  $\mu\text{m}$ . Additionally, the height of the "white water" zone gradually decreases with increasing bubble size.

Current research on flotation tank systems primarily employs two-dimensional (2D) models to investigate the hydrodynamic behavior induced by monodisperse bubbles, typically neglecting bubble coalescence and breakup.

However, whether such a 2D simplification can accurately represent the complex fluid dynamics in practical flotation tanks remains debatable, necessitating a critical evaluation of 2D modeling approaches.

Bubble size critically governs flotation efficiency. Smaller bubbles, while offering greater surface area for particle attachment, require higher quantities to achieve the same flotation capacity, complicating bubble-floc adhesion. Moreover, generating finer bubbles demands elevated system pressure, potentially leading to excessive energy consumption. Conversely, larger bubbles exhibit stronger buoyancy and faster rise velocities, yet their shortened residence time in the tank reduces collision efficiency with flocs, ultimately compromising separation performance<sup>[1,4]</sup>. Thus, a systematic investigation into bubble size effects on hydrodynamic behavior is imperative. With the global push toward "dual-carbon" goals, the resource utilization of CO<sub>2</sub> has gained significant attention. Its high-purity availability further minimizes the introduction of exogenous impurities, reducing system contamination risks.

To address these aspects, this study adopts a population balance model (PBM) to incorporate polydisperse bubbles while accounting for coalescence and breakup dynamics. We evaluate two flotation media—air, carbon dioxide, to elucidate their effects on flow-field characteristics within the flotation tank. Additionally, the influence of initial bubble size on gas holdup in the separation zone is rigorously analyzed.

## 2. Mathematical Modeling Approach

### (1) Turbulence Modeling Methodology

Within flotation tanks, bubble motion significantly modifies the turbulent structure of the liquid phase. The standard k-ε model fails to adequately account for this turbulence modulation, consequently limiting its accuracy in predicting bubble dynamics. Bondelind et al.<sup>[13]</sup> demonstrated that the realizable k-ε model shows superior agreement with experimental measurements, a finding subsequently validated and adopted by numerous researchers<sup>[14-15]</sup>.

Based on these established results, the present study employs the realizable k-ε model coupled with non-equilibrium wall functions for near-wall treatment. The transport equations governing turbulent kinetic energy (k) and its dissipation rate (ε) are formulated as follows:

$$\frac{\partial(\rho k)}{\partial t} + \frac{\partial(\rho k u_i)}{\partial x_i} = \frac{\partial}{\partial x_i} \left[ \left( \mu + \frac{\mu_i}{\sigma_k} \right) \frac{\partial k}{\partial x_i} \right] + G_k + G_b - \rho \varepsilon - Y_M + S_k \quad (1)$$

$$\begin{aligned} \frac{\partial(\rho \varepsilon)}{\partial t} + \frac{\partial(\rho \varepsilon u_i)}{\partial x_i} &= \frac{\partial}{\partial x_i} \left[ \left( \mu + \frac{\mu_i}{\sigma_\varepsilon} \right) \frac{\partial \varepsilon}{\partial x_i} \right] \\ &+ C_{1\varepsilon} \frac{\varepsilon}{k} (G_k + C_{3\varepsilon} G_b) - C_{2\varepsilon} \rho \frac{\varepsilon^2}{k} + S_\varepsilon \quad (2) \end{aligned}$$

Where  $G_k$  represents the generation of turbulent kinetic energy due to mean velocity gradients, kg/(m<sup>3</sup>·s);  $G_b$  denotes the turbulent kinetic energy production from buoyancy effects, kg/(m<sup>3</sup>·s);  $Y_M$  accounts for the contribution of fluctuating dilatation in compressible turbulence kg/(m<sup>3</sup>·s);  $\sigma_k$  and  $\sigma_\varepsilon$  are the turbulent Prandtl numbers for k and ε;  $S_k$  and  $S_\varepsilon$  represent source terms, kg/(m<sup>3</sup>·s).

### (2) Multiphase Flow Modeling Approach

The Eulerian-Lagrangian and Eulerian-Eulerian

frameworks represent the two predominant methodologies in multiphase flow research. The Eulerian-Lagrangian model utilizes a discrete particle method to track individual bubble trajectories while accounting for bubble-bubble and bubble-liquid interactions. This approach is particularly suitable for systems containing relatively low bubble populations with larger bubble sizes (typically >1 mm). However, in dissolved air flotation (DAF) systems where high-density populations of micron-scale bubbles (typically 10-100 μm) are present, the Eulerian-Lagrangian model demonstrates several critical limitations. In contrast, the Eulerian-Eulerian model offers distinct advantages for DAF system simulation. These superior capabilities have led to the Eulerian-Eulerian approach becoming the established standard in flotation research, as evidenced by its widespread adoption in published studies. This formulation's demonstrated reliability for microbubble-dominated flows justifies its selection as the primary modeling framework for the current investigation.

### (3) Population Balance Modeling Methodology

The Population Balance Model (PBM) has been extensively employed to characterize the quantity, size distribution, and dynamic evolution of discrete phase elements (e.g., bubbles, droplets) in multiphase flow systems. This modeling approach fundamentally represents:

$$\frac{\partial}{\partial t} (\rho n_i) + \nabla \cdot (\rho n_i \mathbf{u}) = \frac{\partial}{\partial x_j} \left( D_{ij} \frac{\partial n_i}{\partial x_j} \right) + S_i \quad (3)$$

Where  $n_i$  indicates the concentration of the  $i$ th particle in the particle distribution function within the population balance framework, the concentration of the  $i$ -th particle class in the distribution function Mol/L;  $\rho$  is fluid density, kg/m<sup>3</sup>;  $\mathbf{u}$  is velocity vectors, m/s;  $D_{ij}$  is diffusion coefficient;  $S_i$  is source item.

## 3. The Application Value of Traditional Embroidery in Modern Fashion Design

This study constructed a three-dimensional full-scale air flotation tank model. In the three-dimensional model, the water inlet of the air flotation tank, the release device and the outlet on the outlet pipe are regarded as square openings. To overcome the influence of uneven inlet velocity distribution, a virtual inlet with a length of 20 cm is introduced in the original model. In addition, the outlet holes are set on the side of the outlet pipe to prevent the outlet pipe from being blocked.

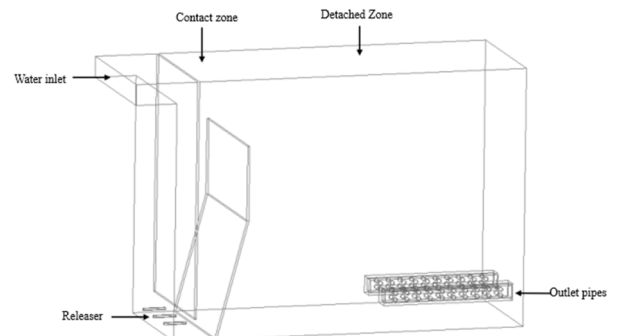


Figure 1. Model of the DAF tank

The ANSYS Fluent software is used to simulate the flow field within the dissolved air flotation (DAF) tank. In this simulation, the inlet of the DAF tank is for liquid-phase water, the inlet of the releaser is for dissolved air water, and the purified water flows out from the water outlet holes on the outlet pipe. A relatively high fluid velocity is conducive to increasing the turbulence intensity, which in turn promotes the collision and adhesion between bubbles and impurity flocs. However, an excessively high fluid velocity may lead to the breakage or detachment of bubbles on the gas-carrying flocs. Meanwhile, it may also cause the gas-carrying flocs to be directly discharged from the outlet pipe along with the water flow, thereby reducing the efficiency of the dissolved air flotation process. Through numerous experiments and simulation analyses, most of the current operations are carried out under the conditions where the inlet velocity of the liquid-phase water is 0.043 m/s and the inlet velocity of the dissolved air water is 2.5 m/s [14,17]. To comprehensively consider the coalescence and breakage behaviors of bubbles, the Population Balance Model (PBM) is introduced [18]. The free liquid surface in the separation zone is in communication with the atmosphere, and the gas phase will disperse into the surrounding air. Therefore, the degassing boundary is adopted for the free liquid surface in the separation zone [19]. In addition, to take into account the influence of gravity, a gravitational acceleration of 9.81 m/s<sup>2</sup> is set in the negative direction of the y-axis. Table 2 lists the boundary conditions and parameters.

**Table 1.** Boundary conditions and parameters

variable	Boundary conditions	value
Water inlet	Speed inlet	0.043 m·s <sup>-1</sup>
Releaser	Speed inlet	2.5 m·s <sup>-1</sup>
Water outlet	Pressure outlet	-
Wall and baffles	Wall boundary	-
Free liquid level in the separation zone	Degassing boundary	-
Contact zone surface	Wall boundary	-

## 4. Results and Discussion

The gas holdup is one of the important indicators for evaluating the effect of dissolved air flotation, which reflects the quantity of microbubbles. Specifically, under the condition that the bubble size is fixed, a higher gas holdup indicates a greater number of bubbles in the dissolved air flotation tank. Correspondingly, the gas-solid ratio will be higher, and the probability of adhesion between bubbles and impurity flocs will also be higher, thereby enhancing the effect of dissolved air flotation.

When air is used as the dissolved air flotation medium, the distribution of gas holdup in the separation zone under different working conditions is shown in Figure 3. As can be seen from Figure 3, the gas holdup varies significantly with height under different working conditions. When the initial bubble size is less than 75 μm, the gas holdup in the area below 0.25 m rises sharply with the increase in height, and then the rate of increase decreases significantly. However, when the height exceeds 1.0 m, the gas holdup decreases. When the initial bubble size is in the range of 1-25 μm, the gas holdup at the bottom of the dissolved air flotation tank is

relatively high. This may cause bubbles to entrain impurity flocs and escape from the outlet pipe, which has an adverse effect on the dissolved air flotation effect. When the initial bubble size is in the range of 25-50 μm, the gas phase is mainly distributed in the upper and middle parts of the separation zone, which is conducive to the rise of bubbles adhering to impurity flocs to the top of the separation zone, thus achieving a better dissolved air flotation effect. When the initial bubble size is greater than 75 μm, the gas holdup is almost zero from the bottom of the separation zone to 0.7 m, and then it rises rapidly. When the initial bubble size is in the range of 100-125 μm, the gas holdup at the bottom of the separation zone is low, and the maximum gas holdup is also smaller compared with other working conditions, being only 3.49 ml/L (gas-water ratio), which is significantly lower than that of other working conditions. This is because larger bubbles have a greater buoyancy in the liquid, and they are likely to float to the upper layer of the separation zone and gather at the free liquid surface of the separation zone, and then disperse into the atmosphere. In conclusion, when air is used as the dissolved air flotation medium, the best dissolved air flotation effect can be achieved when the initial bubble size is in the range of 25-50 μm, while an initial bubble size greater than 75 μm will significantly affect the distribution of the gas phase in the separation zone.

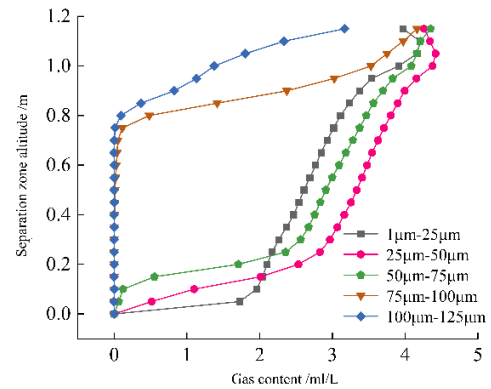


**Figure 3.** Distribution of air concentration against height with various initial bubble sizes

Figure 4 illustrates the distribution of gas holdup in the separation zone under different operating conditions when using carbon dioxide as the flotation medium. As shown in Figure 6, the gas holdup distribution follows a similar trend to that observed with air as the flotation medium.

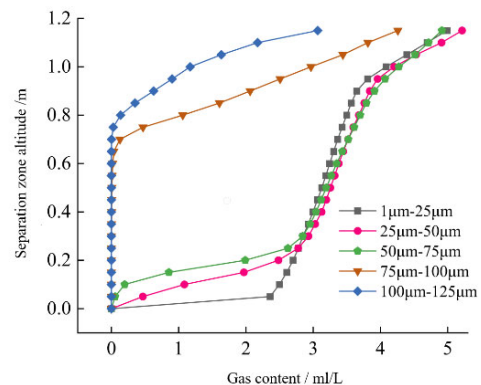


**Figure 4.** Distribution of carbon dioxide concentration against height with various initial bubble sizes

When the initial bubble size exceeds 75  $\mu\text{m}$ , the lower region (below 0.7 m) exhibits negligible gas presence, followed by a rapid increase to the maximum gas holdup, which remains relatively lower compared to other conditions. In contrast, when the initial bubble size is below 75  $\mu\text{m}$ , the gas phase predominantly accumulates in the middle-upper section of the separation zone. Specifically, for initial bubble sizes ranging from 1 to 25  $\mu\text{m}$ , the gas holdup reaches 2.36 mL/L at a height of 0.05 m, representing a 36% increase compared to the case where air is used as the flotation medium.

For initial bubble sizes smaller than 75  $\mu\text{m}$ , the gas holdup remains nearly uniform above 0.3 m, with no anomalous reduction observed near the liquid surface of the flotation tank. The maximum gas holdup under these conditions is significantly higher (4.91–5.21 mL/L) than that achieved with air as the flotation medium. These findings suggest that optimal flotation performance is achieved when using carbon dioxide with an initial bubble size between 25 and 75  $\mu\text{m}$ .

## 5. Conclusion

This study investigated gas holdup distribution characteristics in flotation separation systems through comprehensive two-phase flow simulations within a dissolved air flotation (DAF) tank. The reliability of three-dimensional modeling predictions was rigorously evaluated and validated against experimental data from Lundh et al. Subsequently, systematic examinations were conducted to analyze the influence of initial bubble size on gas holdup distribution patterns under various flotation media conditions, yielding the following key findings:

a) The optimal bubble size range for flotation performance was found to be intrinsically dependent on the physical properties of the gas medium. A clear correlation was observed between the gas medium density and the optimal bubble size range, with the required bubble diameter increasing progressively with higher gas density. Specifically, the experimentally determined optimal initial bubble size ranges were: 25–50  $\mu\text{m}$  for air, and 25–75  $\mu\text{m}$  for carbon dioxide, especially.

b) The gas holdup profiles exhibited remarkably similar height-dependent trends when using air, carbon dioxide as flotation media. In terms of overall performance, the air flotation system with carbon dioxide as the flotation medium showed the lower overall performance

## References

- [1] Wang G, Ge L, Mitra S, et al. A review of CFD modelling studies on the flotation process[J]. *Minerals Engineering*, 2018, 127: 153-177.
- [2] Sancho I, Lopez-Palau S, Arespachaga N, et al. New concepts on carbon redirection in wastewater treatment plants: A review[J]. *Science of the Total Environment*, 2019, 647: 1373-1384.
- [3] Al-Shamrani A A, James A, Xiao H. Separation of oil from water by dissolved air flotation[J]. *Colloids and surfaces A: Physicochemical and engineering aspects*, 2002, 209(1): 15-26.
- [4] Edzwald J K. Dissolved air flotation and me[J]. *Water research*, 2010, 44(7): 2077-2106.
- [5] Satpathy K, Rehman U, Cools B, et al. CFD-based process optimization of a dissolved air flotation system for drinking water production[J]. *Water Science and Technology*, 2020, 81(8): 1668-1681.
- [6] Kwon S B, Park N S, Lee S J, et al. Examining the effect of length/width ratio on the hydro-dynamic behaviour in a DAF system using CFD and ADV techniques[J]. *Water science and technology*, 2006, 53(7): 141-149.
- [7] Tang J, Long Y, Fu Y, et al. Numerical investigation of the multiphase flow patterns and removal effect in a large dissolved air flotation[J]. *Water Quality Research Journal*, 2022, 57(3): 123-139.
- [8] Berrío J C, López J, Cristancho P, et al. Evaluation of a Dissolved air flotation system for different operating conditions[J]. *Revista de Ingeniería*, 2014 (41): 46-52.
- [9] Wang Y L, Wang N, Jia R, et al. Research on CFD numerical simulation and flow field characteristics of countercurrent–cocurrent dissolved air flotation[J]. *Water Science and Technology*, 2018, 77(5): 1280-1292.
- [10] Kiuri H J. Development of dissolved air flotation technology from the first generation to the newest (third) one (DAF in turbulent flow conditions)[J]. *Water Science and Technology*, 2001, 43(8): 1-7.
- [11] Deng B, Ding Q, Ge D. Three dimensional Eulerian-Eulerian simulation on hydrodynamics in dissolved air flotation tank with different turbulence models[J]. *Water Science and Technology*, 2017, 76(2): 425-433.
- [12] Chen A, Wang Z, Yang J. Influence of bubble size on the fluid dynamic behavior of a DAF tank: a 3D numerical investigation[J]. *Colloids and Surfaces A: Physicochemical and Engineering Aspects*, 2016, 495: 200-207.
- [13] Bondelind M, Sasic S, Kostoglou M, et al. Single-and two-phase numerical models of Dissolved Air Flotation: Comparison of 2D and 3D simulations[J]. *Colloids and Surfaces A: Physicochemical and Engineering Aspects*, 2010, 365(1-3): 137-144.
- [14] Rodrigues J P, Batista J N M, Béttega R. Application of population balance equations and interaction models in CFD simulation of the bubble distribution in dissolved air flotation[J]. *Colloids and Surfaces A: Physicochemical and Engineering Aspects*, 2019, 577: 723-732.
- [15] Tang L, Zhang S, Li M, et al. Numerical investigation on the dynamic flow pattern in a new wastewater treatment system[J]. *Water*, 2021, 13(8): 1101.
- [16] Ström H, Bondelind M, Sasic S. A novel hybrid scheme for making feasible numerical investigations of industrial three-phase flows with aggregation[J]. *Industrial & Engineering Chemistry Research*, 2013, 52(29): 10022-10027.
- [17] Amato T, Wicks J. The practical application of computational fluid dynamics to dissolved air flotation, water treatment plant operation, design and development[J]. *Journal of Water Supply: Research and Technology—AQUA*, 2009, 58(1): 65-73.
- [18] Lakghomi B, Lawryshyn Y, Hofmann R. Evaluation of flow hydrodynamics in a pilot-scale dissolved air flotation tank: a comparison between CFD and experimental measurements[J]. *Water Science and Technology*, 2015, 72(7): 1111-1118.
- [19] Lee K H, Kim H, Kuk J W, et al. Micro-bubble flow simulation of dissolved air flotation process for water treatment using computational fluid dynamics technique [J]. *Environmental Pollution*, 2020, 256: 112050.